Sensors and Actuators A 319 (2021) 112526

Contents lists available at ScienceDirect

Sensors and Actuators A: Physical

journal homepage: www.elsevier.com/locate/sna

Low-cost microfluidic device micromachining and sequential integration with SAW sensor intended for biomedical applications

S. Stoukatch [a,*], L.A. Francis [b], F. Dupont [a], M. Kraft [a,c,1]

[a] Microsys Lab, Department of Electrical Engineering and Computer Science, Liege University, Liege Scientific Park, Rue du Bois Saint Jean 15-17, B-4102, Seraing, Belgium
[b] Institute of Information and Communication Technologies, Electronics and Applied Mathematics (ICTEAM), Université Catholique de Louvain, 3, Place du Levant, B-1348, Louvain-La-Neuve, Belgium
[c] Department of Electrical Engineering (ESAT) – MICAS, Microelectronics and Sensors, University of Leuven (KUL), Leuven, Belgium

ARTICLE INFO

Article history:
Received 15 July 2020
Received in revised form
24 November 2020
Accepted 18 December 2020
Available online 12 January 2021

Keywords:
Microfluidic device manufacturing
Microfluidic biosensing system
Low cost manufacturing
Low temperature integration
Biomedical application
Surface acoustic wave sensor

ABSTRACT

The paper reports on fabrication processes related to low-cost manufacturing and integration of microfluidic biomedical detection systems fabricated without a cleanroom. First, we developed and demonstrated a process for manufacturing a microfluidic device. Second, we demonstrated a low temperature assembly technique for the packaging of the surface acoustic wave (SAW) sensor die. Sequentially, we demonstrated a low temperature process for the integration of the microfluidic device with a SAW sensor to form a fully functional biomedical detection system. The microfluidic device was manufactured by mechanical micromilling technology that is rapid, conceptually simple and a low-cost process. It is suitable for both prototyping and for a low and a medium scale production to address a niche market that is typical for the intended application. That technology has no specific requirement for a certified clean room environment. Unlikely other technology, such as molding and photolithography, for example, it has a shorter lead-time from design to manufacturing. The assembly technique for a SAW sensor is a carefully selected combination of known and matured processing steps causing no damage to a sensitive biofunctionalization on the sensor. The developed and demonstrated integration process for the in-house manufactured microfluidic device and the SAW sensor is a purely low temperature process that prevents a biological material deposited on the SAW sensor from degradation. Biocompatibility issues were also addressed during the study reported. Finally, we performed an ultrasonic (US) impedance characterization of the fully assembled system and demonstrated that neither the microfluidic system integrated on the sensor nor the integration process itself have an impact on the US impedance of the SAW sensor. That means that it does not affect the sensor performance.

1. Introduction

There are numerous publications about surface acoustic wave (SAW) sensors for biochemical analyses, Gronewold [1] reviewed trends and challenges in SAW sensors; Gizeli and Lowe [2] examined publications on the acoustic transducers, physics transducers and use them for biological analyses; Bracke et al. [3] evaluated the performance of the SAW biosensor technique from a pharmaceutical quality point of view; Go et al. [4] published a comprehensive review on recent advances in SAW devices for chemical sensing and microfluidic processing ; Wang et al. [5] demonstrated the three-dimensional finite element model for SAW sensors. Our project consortia ICTEAM, UCL published several works on the topic, for example Friedt and Francis [6] demonstrated SAW combining device for thin layers characterizations; Fissi et al. [7] developed a fabrication process for the SAW device; Fissi et al. [8] demonstrated the fluidic analyses using the SAW device. They proved that SAW sensors in principle, are suitable for in-liquid biochemical analyses.

Still, there are several challenges on how to build a fully integrated functional biomedical detection system from an individual bare-die SAW sensor. A first challenge is how to apply the test specimen to the sensing area of the SAW sensor. Typically, a micro-fluidic system is used for that, which must be developed, manufactured and fully integrated with the SAW sensor. The fluidic system, beyond simple functionality must meet several specifications, the most essential are: i) not to affect the acoustic impedance

* Corresponding author.
E-mail address: serguei.stoukatch@uliege.be (S. Stoukatch).
[1] He is currently with Department of Electrical Engineering (ESAT) – MICAS, Microelectronics and Sensors, University of Leuven (KUL), Leuven, Belgium.

https://doi.org/10.1016/j.sna.2020.112526
0924-4247/

of the SAW sensor, ii) to be biocompatible to liquid samples, iii) to be easily integrated and causing no damage or changes of functionality of the SAW sensor during the integration process. Furthermore, the fluidic system should be cheap, easy to design, having a short time lead time from design to manufacture, and finally easy to manufacture. Considering the dimensions of the micromachined SAW sensor, a microfluidic system can potentially fulfill these requirements. Stoukatch [9] reported on several technologies that are readily available to manufacture such a microfluidic device. According to the review performed by Wu et al. [10] the most popular methods are based on photolithography, injection molding and PDMS casting. This typically requires a customized mask set for photolithography and clean room environment. The injection molding needs an expensive molding chase. For medium-scale production, these NRC (non-recurring cost) can be significant and are only negligible for mass-scale production. The PDMS (polydimethylsiloxane, a silicon-based organic polymer) casting according to Wu et al. [10] and a review performed by Sackmann et al. [11] is widely used for research purpose and prototyping runs as proof of concept devices. Although according to Sackmann et al. [11], it is not only an expensive material, it has numerous limitations to using the material in biomedical devices. M. Grösche et al. in their paper [12] evaluated different manufacturing processes including stereo lithography and micromilling for typical microfluidic applications.

Another challenge for manufacturing an integrated biomedical detection system is how to package a biofunctionalized SAW sensor and integrate it with the microfluidic system without damaging its sensitive bio-layer. The biofunctionalized SAW sensor must be packaged and the system to supply a liquid specimen (microfluidic system) for bioassay must be developed and integrated. Van Loo et al. [13] reported that the biofunctional layer is sensitive to chemical exposure and thermal treatment that are typically taking place during processing steps required for the assembly and integration. By chemical exposure, we understand any contact with any liquid chemical, including water. The thermal treatment must be limited in terms of temperature applied and the overall duration of the thermal exposure.

As a solution, we used low and/or lower than conventional temperature assembly and integration techniques, as described in the following.

In this work, we developed an integrated microfluidic biomedical detection system that is intended for the immunological detection of bacteria in complex liquids. The examined liquid is supplied to the biofunctionalized SAW sensor by the microfluidic system. In this work, we used a SAW sensor fabricated by our project partners ICTEAM, UCL (Fissi et al., [7] and Fissi et al. [8],) demonstrated theirs functionality. The focus of this work was i) to design and process without the requirement of a cleanroom a low acoustic impedance microfluidic system, ii) to package a thermo-sensitive biofunctionalized SAW die, iii) to integrate the manufactured fluidic system with the biofunctionalized SAW sensor and to perform a basic functional characterization of the fully integrated system.

2. SAW sensor die

The SAW sensor dies processed on 3q̈uartz wafer of 0.3 mm thick at the WinFab, UCL. After fabrication the wafer was singulated into individual SAW dies that can be sequentially biofunctionalized. The individual bare SAW sensor die had 17×6.7 mm^2 lateral dimensions and 0.3 mm thickness, as presented in Fig. 1.

The SAW sensor die comprises two pairs of IDT (interdigitated electrodes) and a sensing area in between. Each IDT comprises of 50 pairs of 4-finger electrodes of 0.2 μm thick aluminum layer. The acoustic wave is excited by the emitting IDT, transmitted via the propagation part (the sensing area), and then detected by the receiving IDT. The wavelength is about 40 μm and a resonance frequency is 125 MHz. The insertion loss and the phase change was measured for a specimen of different concentration in a liquid solution. The receiving IDT detects the changes, then recorded and correlated to a specific concentration of complex elements. The biofunctionalization of the sensing area makes it sensitive to specific biological elements in-liquid, such for example bacteria in complex liquids for an immunological detection.

3. Assembly

3.1. Adhesives

Special attention was paid to the selection of suitable adhesives, which were used for several assembly steps, such as mounting the SAW sensor die to the PCB, wire bond encapsulation and mounting the microfluidic channel to the SAW sensor.

The adhesive must meet several criteria. As the interconnect material, it must provide sufficient mechanical strength without causing any damage to the interconnected parts. Furthermore, it must cure at low or at lower than a conventional adhesive cure temperatures (150 °C as stated by Stoukatch [9]) and cause no damage to thermal sensitive parts of the assembly. Additionally, the adhesive being a part of the biomedical device must meet the required criteria for biocompatibility. The adhesive used for bond-wire encapsulation must initially have low viscosity and after curing low elasticity in order not to compromise the bond-wire integrity.

Based on previous work (Van Loo et al., [13]), we selected non-conductive electronic adhesives (NEA) 121, 123 from Norland Products Inc. Cranbury, NJ, USA (further in the text, NEA 121 or NEA 123). Both are from the same family of adhesives and have a proprietary chemical formulation, based on mercaptoester with a concentration of 20–60 % and up to 3 % urethane. NEA 121, 123 are single component solvent free adhesives that form cross-linking under exposure to UV light. They are sensitive to the whole range of UV light from 320 to 380 nm with a peak sensitivity around 365 nm. For full curing 3 joules/cm^2 (NEA121) and 4.5 joules/cm^2 (NEA123) UV energy is required. The cure time depends on the light intensity, wavelength and thickness of the adhesive layer and varies in the range from 5 to 30 s for half inch thickness. The adhesive also contains a heated catalyst that can help to cure areas unexposed to UV light. The adhesives can be thermally cured (without UV exposure) at 125 °C in 10 min in a convection oven, or at 80 °C in 3 h. A temperature less than 60 °C will not activate the adhesive cure. The advantage of the heat cure is to cure partially UV exposed areas fully. The adhesives viscosity varies in a broad range from low to high viscosity that enables different applications. Once the NEA 121 and 123 are fully cured, they form a clear, colorless and inert material with excellent mechanical properties. The physical properties of NEA 121 and 123 adhesives can be accessed on (Norland Electronic Adhesives). NEA121 is a low viscosity adhesive, easy to apply on the designated area; it is a stiff material after a full cure and used as an attach adhesive. NEA123 M and T are softer than NEA121, and used for encapsulation of wire bonds.

It is well known (Li and Zhou, [14], that polyurethane and mercaptoester based adhesives are widely used for biomedical device manufacturing; in fact, they are approved as a component of biomedical devices. For example, Tang et al. [15] grew living cells on a mercaptoester-based layer. The majority of such adhesives will pass biocompatibility testing, although each specific adhesive must be individually tested against for specific biocompatibility, reflecting the intended use of the device.

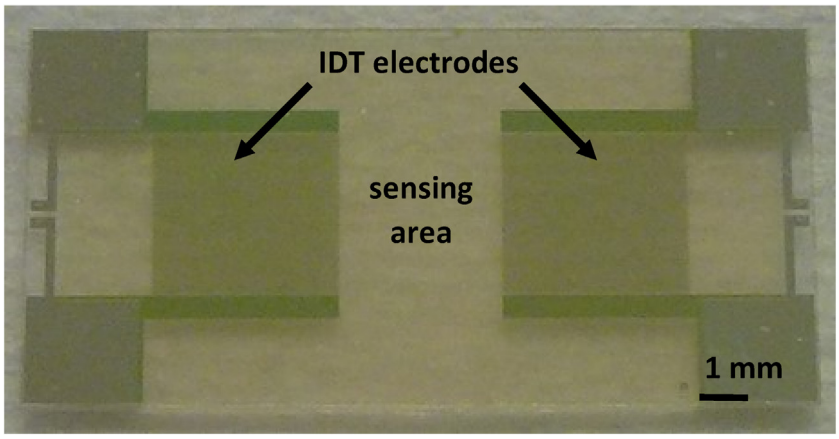

Fig. 1. Top view of a singulated SAW sensor die.

3.2. SAW sensor die mounting

We designed a PCB to support a SAW die sensor mechanically and connected it electrically to a readout electronics (Fissi et al., [7]). The PCB comprises a mounting area for the SAW sensor die, wire bonding pads to interconnect electrically the sensor using the wire bonds to the PCB, mounting pads for the connector to connect the PCB with cables to enable electrical characterization of the assembled system. The PCB design also allows to perform an electrical characterization directly of the mounted SAW sensor.

On the next step, we mounted the SAW sensor die on the PCB; for that, we used the non-conductive electronic adhesive NEA 121.

First, we dispensed a layer of 30 μm thick adhesives NEA 121 at a designated area of the PCB, then aligned the SAW sensor die to the PCB mounting area, then brought it in contact with the adhesive and pressed it with a load of 10 N. For that, we used a manual pick and place system equipped with an optical microscope. After that, we cured the adhesives. The SAW sensor die on a quartz substrate is transparent for the UV light, and to cure the adhesive thus we used the UV spot curing system OmniCure^{TM} Series 1000 with a flexible light guide from Excelitas Technologies (UV Omni Cure). The system is equipped with a powerful high-pressure 100 W mercury vapor short arc lamp. The maximum intensity of the UV exposure provided by the system is 18.5 W/cm^2 of irradiance output. For the NEA 121 adhesives cure, we selected a bandpass of 365 nm wavelength. The adhesives was cured at a maximum exposure time of 20 s. In our previous work (Van Loo et al., [13]), we have shown that such UV exposure (dose of exposure and maximum insensitivity) causes no direct damage to the biofunctionalized layer on the sensor.

3.3. Wire bonding

Once the SAW sensor is permanently mounted to the PCB, we interconnected the die electrically to the PCB using wire bonding. According to Harman [16], gold or copper wire bonding is currently two main bonding techniques that contribute up to 90 % of the commercial market. However, they require a high bonding temperature, at least 150 °C for the gold bonding, and up to 220 °C for copper bonding. Therefore, the workpieces are subjected during the wire bonding process to an elevated temperature for a prolonged period of time. It is acceptable for ASICs and some MEMS sensors, but definitely will cause irreversible damage for a biosensitive layer.

Therefore, for the electrical interconnection of the SAW sensor die, we choose an alternative wire bonding technique, namely aluminum (Al) wedge-wedge wire bonding. The main advantage of that technique is that it works at room temperature.

To perform the Al wire bonding (wire diameter of 25 μm), we used a semi-automatic HB 16 wire bonder from TPT, Germany. The system is equipped with a 64.1 kHz frequency transducer of 3 W maximum output. A work holder temperature was set to 20 °C and was constant during all experiments.

Directly after the wire bonding, we encapsulated the bonded wire. For that we used the high viscosity dam encapsulant NEA 123 T and the low viscosity NEA 123 M fill encapsulant. They are from the same family of adhesives as NEA 121. The purpose of the encapsulation is to protect the wires against an environmental impact such as mechanical damage, contamination, humidity and corrosion, and other factors. After the wire bond encapsulation, the assembly can be easily handled without the risk of being damaged during transportation.

4. Microfluidic system

The function of the microfluidic system is to supply the test specimen onto the sensitive part of the biofunctionalized SAW die for a biological assay, to remove the test specimen afterward, finally to purge it by a neutral liquid solution to prepare the sensor for the next assay.

4.1. Microfluidic channel architecture

The inner dimension of the microfluidic channel is defined by the overall area of the active part (sensing part) of the SAW sensor and equal to 3.0 mm x 8.0 mm.

The mounting area for the microfluidic channel is marked by thick red line. Another essential requirement is that the inner wall of the channel must be relatively narrow in order not to change the acoustic impedance of the SAW sensor. Previous research (Fissi et al., [7]) demonstrated that the wall thickness less or equal to 250 μm is acceptable to ensure an adequate SAW sensor performance. Insertion losses for various wall thickness deposited on the acoustic part were measured. Presence the wall increases the insertion losses from -22 dB (no wall) to -45 dB (for 250 μm wall), which is regarded as a maximum acceptable loss for the device performance.

Therefore, a wall thickness of 250 μm the maximum value for the acoustic part of the SAW sensor that will not change the acoustic impedance and will not significantly disturb the SAW wave propagation above the specified limit. Thinner than 250 μm walls are better for device performance. On another hand, it is more difficult to process the thinner wall in a repeatable way because of specific process limitations. In addition to the described manufacturability

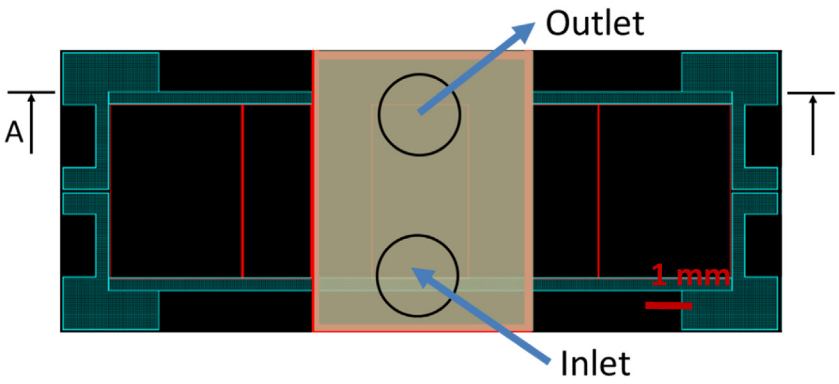

Fig. 2. Layout of the microchannel: top view.

Fig. 3. Layout of the microchannel: cross-sectional view.
Legend to Fig. 3:
W: wall thickness.
H: the total thickness of the microfluidic channel.
D: depth of the microfluidic channel.

issues, the wall has a function of a jointing part for the microfluidic channel. The wall thickness defines a contact area between the microfluidic channel and the SAW die. In order to achieve a minimal shear strength of 6.89 MPa that corresponds to 2.5 kg force according to standard described in Die Shear Strength, MIL-STD-883 F, Method 2019.7 [17], we need at least 150 μm thick wall.

The construction of the microfluidic channel is illustrated in Figs. 2 and 3.

The microfluidic channel comprises inlet and outlet openings on a top part of the channel. The inlet and outlet both have a 2 mm diameter. The depth of the channel is 0.55 mm. The total nominal volume of the microfluidic channel is 0.0132 mL (13.2 μL). Taking into account the tolerance of the actual geometry of the channel, the volume can vary from 12.6 μL to 13.8 μL.

4.2. Microfluidic channel fabrication

4.2.1. Out of clean room microfluidic channel fabrication

In the introduction to this paper, we mentioned the most common techniques of microfluidic channel processing, most of them require a cleanroom environment. To process the specific microfluidic channel we considered several micromachining techniques, with a focus on low cost and low entry technologies and that have no cleanroom requirements. The process was based on conventional techniques such as dispensing, molding and micromilling. The main challenge was to make the walls of the microfluidic channel thinner than the specified thickness of 250 μm, keeping in mind that a thinner wall will be an advantage and the lowest limit of 150 μm.

The dispensing technique comprises dispensing of the adhesive and sequential curing it to form walls of the microfluidic channel, then mounting a plastic plate on top of the adhesive walls to form a top part of the channel. Here, the main issue was to reach a required wall height while keeping its width below 250 μm; for this, at least 3 or preferably 4 passes of adhesive dispensing was required. However, this resulted in a significant wall height deviation within a single device.

We also explored a molding technique. This technique, instead of processing walls of the microfluidic channel by dispensing, forms the walls by casting a liquid material into a pre-processed mold, curing it and removing the formed mold piece. We reached a wall width of 200 μm with uniform wall height. The problem here was how to remove the processed frame out of the mold. Apparently, the material was not stiff enough to withstand the removal process and the frame always broke at the longer side of the frame.

Finally, we explored a micromilling technique using a entry-level low cost VISIO F machine, from Sigea, France, which is a 3-axis CNC micromilling machine, a vertical system.

4.2.2. Out of clean room microfluidic channel fabrication using micromilling technology

The function of the microfluidic channel is to deliver a liquid bio-specimen to the active area of the sensor. It means that the microfluidic channel comes in direct contact with bio-species that dictates requirements for specific biological and chemical properties. The material must be biocompatible to the levels required for the specific use. The requirement for meeting specific chemical properties is typically understood as to be resistant to solvents used in life sciences applications. Stoukatch [9] reported on several materials as polyimide, cyclic olefin copolymer (COC), PMMA and polycarbonate (PC) for example that meet the required specifications and that can be micromachined by milling.

As a material to process a microfluidic channel, we finally selected a polycarbonate (PC). It is a transparent material and has an interesting combination of the thermo-mechanical properties; it is also suitable for micromilling processing and is relatively inexpensive. The thermo-mechanical properties of the PC are presented in our previous publication (Stoukatch [9]). Due to the biocompatibility of PC and its chemical resistance, is often used for biomedical device manufacturing. It shows no interaction with the majority of materials used for biomedical applications and life science, such as water, ethanol, ethylene glycol, glycerol (Stoukatch [9]) and withstands multiple cycles of sterilization.

Based on the specifications defined in the Section M̈icrofluidic channel architecture,ẅe designed the microfluidic channel for processing by micromilling. For manufacturing, we used 1 mm thick PC sheets, cut it by the micromilling machine into individual workpieces of 3.4 mm x 8.4 mm and then processed the cavity inside the PC workpieces. For that, we used the following parameters and tooling: 0.5 mm diameter milling tool, rotation of 20,000 rpm, and a feed speed 1 mm/sec. We tried also smaller than 0.5 mm milling tools, as 0.1 mm and 0.2 mm diameter. However, they require low then 0.5 mm/sec feed speed. The larger tool, the tool diameter of 1 mm did not provide us a required micromachining precision and

Fig. 4. Perspective view on a processed microfluidic channel. W: wall thickness and d: depth of the microfluidic channel.

Table 1
Wall thickness of the microfluidic channel.

Set #	Design value, μm	Actual value, μm
1	250	190–230
2	200	165–200

resulted in rougher surfaces. After the microfluidic channel processing, we drilled two circular openings of 2 mm diameter for an inlet and an outlet. The processed and cleaned microfluidic channel is presented in Fig. 4.

The micromilling with the develop configuration allows to process up to 20 microfluidic channels within 1 h. Such throughput is suitable for both prototyping and as well as for low and medium scale production. It fulfills a niche market for the intended application. That technology has no specific requirement for a certified clean room environment. After manufacturing, the specimens were washed and introduced into the clean room for further processing.

4.3. Microfluidic channel characterization

Besides the microfluidic channel appearance, we controlled several critical parameters such as the channel depth (d), the wall thickness (W), and roughness inside the channel cavity. We controlled the wall quality and measured the wall thickness using a Leica Z6APO optical microscope, a magnification to 225 × . We processed two sets of microfluidic channels; sample #1 had a wall thickness of 250 μm and sample #2 had a thickness of 200 μm. Using the optical microscope we also measured the actual thickness of the microfluidic channel's walls (Table 1).

The actual thickness of the walls was systematically less than programmed on the machine on all processed samples. However, such dimensional deviation is in line with the micromilling machine accuracy.

For the roughness measurement, we used a stylus type profilometer from Bruker, model Dektak XT.

The micro-roughness scan was performed on each sample in the middle of the microfluidic cavity (between inlet and outlet). A result of the profilometry scan on the surface of the microfluidic channel for sample #1 is presented in Table 2.

Based on the roughness characterization, one can conclude that the surface machined by micromilling a relatively smooth with Ra of 1.03 μm and suits for our intended application.

4.4. Microchannel integration

Once the microfluidic channel was manufactured and characterized, it had to be mounted on the designated area of the SAW sensor to form a fully integrated biomedical detection system.

Table 2
Surface roughness characterization of the test sample #1.

Parameter	Sample #1
Ra, μm	1.03
Rq, μm	1.33
Rp, μm	4.32
Rv, μm	3.10
Rmax, μm	7.42

Abbreviation list:
Ra - arithmetic average of absolute values.
Rq - root mean squared.
Rmax = Rp + Rv, the maximum height of the profile.
Rp – maximum peak height.
Rv - maximum valley depth.

First, we dispensed a 30 μm thick layer of a low viscosity adhesive NEA 121 on a flat substrate, then using a die bonder PP6 we dipped the microfluidic channel inside the adhesive layer, after that, we dragged that out. During this step, the adhesives transferred from the flat substrate to the mounting surface of the wall. The PP6 series die bonder is a universal semi-automatic system from JPF Microtechnic, France. The die bonder is for accurate mounting semiconductors components on all types of substrate, including a flip-chip bonding capability. The tool placement accuracy is +/−5 μm at 3 sigmas. It can apply automatically programmed bonding force that ranges from 0.1 to 60 N.

On the next step of assembly, using PP6, we aligned the microfluidic channel to the designated area of the SAW sensor die and then bonded them together. The bonding force was set to 2 N. For the permanent fixation of the microfluidic channel, we used a 20 s UV curing by OmniCure. The final assembly is depicted in Figs. 5 and 6.

Once the microfluidic channel was permanently bonded to the SAW sensor die, we checked the hermeticity of the sealing joint between the microfluidic part and the sensor. For that, we injected a red ink through the inlet and then observed the ink spreading visually. We tested all 6 assembled samples, which showed no ink penetration through the sealing. Based on that experiment, we concluded that we established a bonding process that results in a gross-leak secure microfluidic channel (Fig. 7).

The liquid test specimen can be delivered to the microfluidic channel manually by pipette from a 2 mm diameter inlet. In the system, we have also foreseen the automatic delivery option of the test liquid specimen; for that, we build into the inlet and outlet openings a modified microfluidic connector from Microfluidic ChipShop. The mini Luer connector is a single connector type, made from polypropylene (PP), that has a fitting diameter of 1.6–2.0 mm and an outlet diameter of 2.5–2.8 mm diameter that allows it to connect it directly via standard tubes of the corresponding diameter to a feeding instrument.

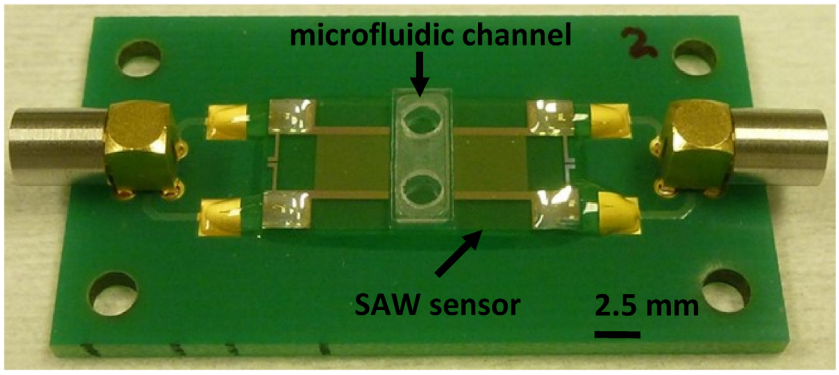

Fig. 5. Top-angle view of the final assembled system.

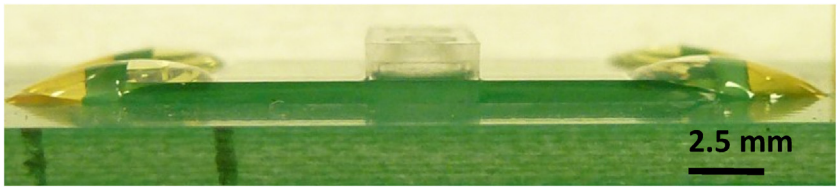

Fig. 6. Angle view of the assembled system.

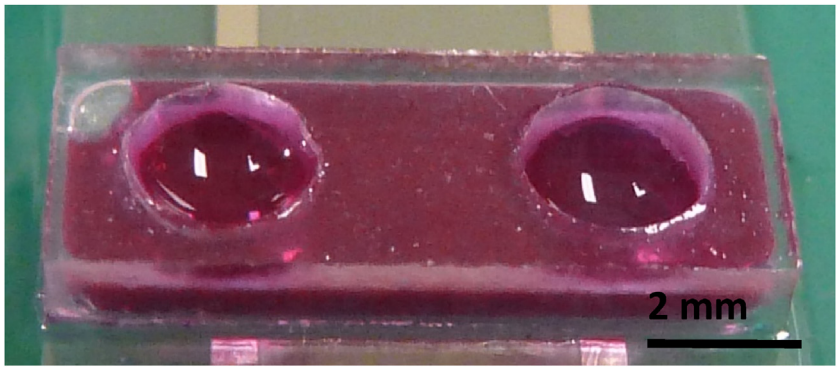

Fig. 7. The gross-leak test: the red ink injected into the microfluidic channel (For interpretation of the references to colour in this figure legend, the reader is referred to the web version of this article.).

This connector is the smallest commercially available; however, the length of the fitting part of the connector is too long to be accommodated on the microfluidic device. Therefore we modified the length of the fitting part, cutting it to a final length of 0.5 mm. For the permanent fixation of the connector to the microfluidic part, we glued it using NEA 121.

5. Electrical characterizations

5.1. Method

As already discussed in section "Microfluidic channel architecture", the microfluidic channel can change the acoustic impedance of the SAW sensor. In this section, we validated this for the microfluidic channel mounted permanently on the SAW sensor. Additionally, we confirmed that the processing steps involved in the assembly of the SAW sensor and sequential integration of the microfluidic channel had little or no impact on the system performance. The SAW sensor bare die was subjected to a variety of sequential assembly steps, such as die mounting, wire bonding, wire bond encapsulation and the microfluidic channel integration. First, we performed acoustic characterization of a bare SAW die, then sequentially repeated the characterization after each assembly step.

5.2. Measurement set-up

For acoustic impedance characterization, we used a Vector Network Analyzer (VNA) ZVRE from Rhode & Schwarz (VNA Rhode & Schwarz ZVRE). We measured an amplitude and phase of the acoustic impedance of the test samples in a frequency range from 115 MHz to 135 MHz.

First, we measured each bare SAW sensor with a specially developed measurement set up, that comprised a probe station equipped with a microscope and X, Y, Z table, and a table for probe positioners. The RF probe positioner holds the RF probe with the following characteristics: IZI probe classic, nickel tip, standard body, 350 μm pitch, and a maximum frequency of 10 GHz. The probes were aligned to the corresponding electrode of the SAW sensor die. The probing electrodes were specially designed and processed on each SAW sensor to enable electrical characterization on a bare sensor die. After that, we measured frequency response of each sensor at different stages of the assembly process: a) after mounting the sensor to the PCB and wire bonding, b) after wire bonds encapsulation,

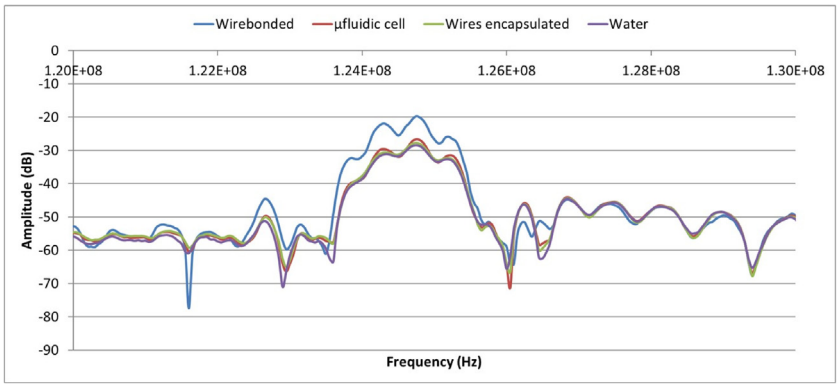

Fig. 8. Amplitude (S21) versus frequency range measured on the SAW sensor (#2) at different stages of the assembly process.

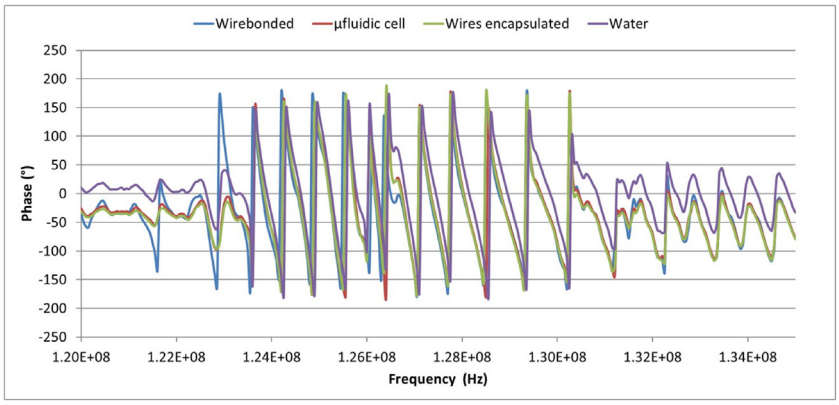

Fig. 9. Phase (S21) versus the frequency range measured on the SAW sensor (#2) at different stages of the assembly process.

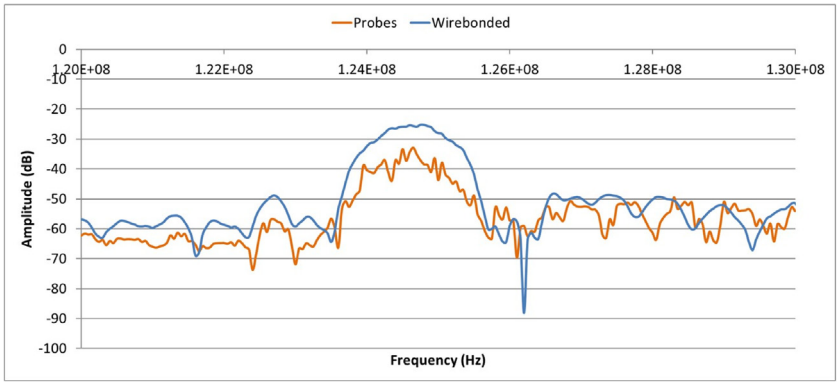

Fig. 10. Amplitude (S21) versus frequency range measured on the SAW sensor (#3) before and after wire bonding.

c) after integration the microfluidic channel with the sensor and finally, d) introduction water into microfluidic channel.

Once the SAW sensor was mounted and wire bonded to the PCB, to perform electrical characterization, there was no need to use a probe station. We connected the assembly to the VNA directly using the cable to the corresponding connector on the PCB.

6. Results

In total, we performed the measurements on 6 test samples. The results show good repeatability. The curves of amplitude and phase versus frequency of all measured spectra for the 6 samples look similar and repeatable.

On step a) the amplitude of the signal in transmission mode (S21) is between -20 and -30 dB. Step b) induces insertion losses of about 10 dB in the frequency range of interest (around 125 MHz). Steps c) and d), on the other hand, cause little or no impact. Besides, the phase remains linear, which is valid even after step 4. Figs. 8 and 9 show a summary after each step.

For the measurement, the signal obtained using the probes is noisier, whereas the signal on wire-bonded samples is smoother, which is typical behavior. Except that the signals for both amplitude and phase are similar. The results are presented in Figs. 10 and 11.

On the final stage of sample characterization, we studied the impact of the deionized water (DI) on the acoustic impedance characteristics. DI water was chosen as it is a basic solution for biological test specimens to perform a bioassay. We compared the amplitude and phase of the test sample without and with DI water and observed no detectable difference. We also did not detect any changes after 2 and 4 h of the DI water staying in the

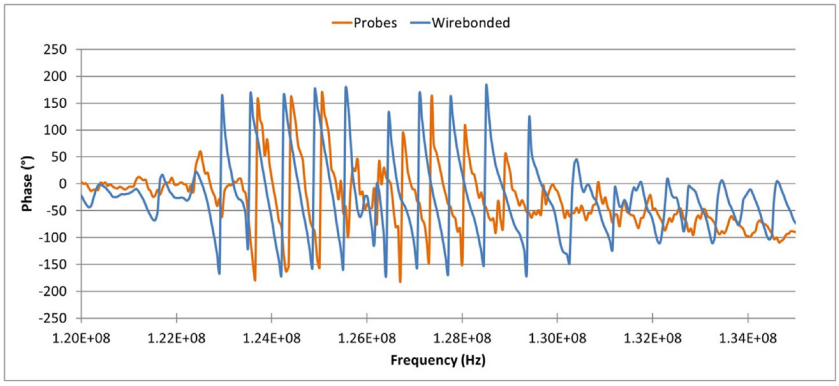

Fig. 11. Phase (S21) versus the frequency range measured on the SAW sensor (#3) before and after wire bonding.

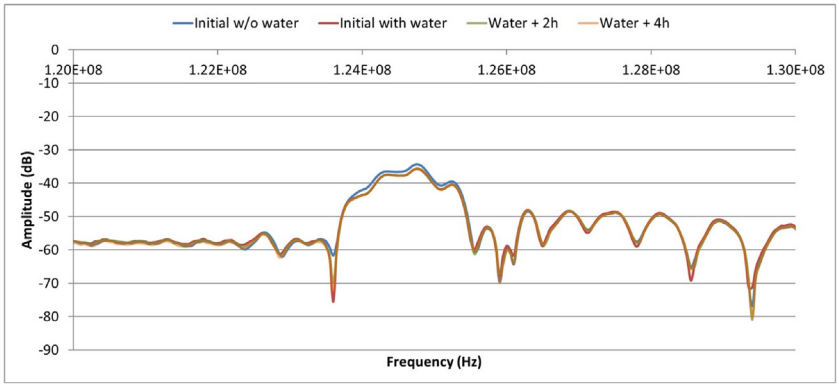

Fig. 12. Amplitude (S21) versus frequency range measured on the SAW sensor (#5) with and without DI water.

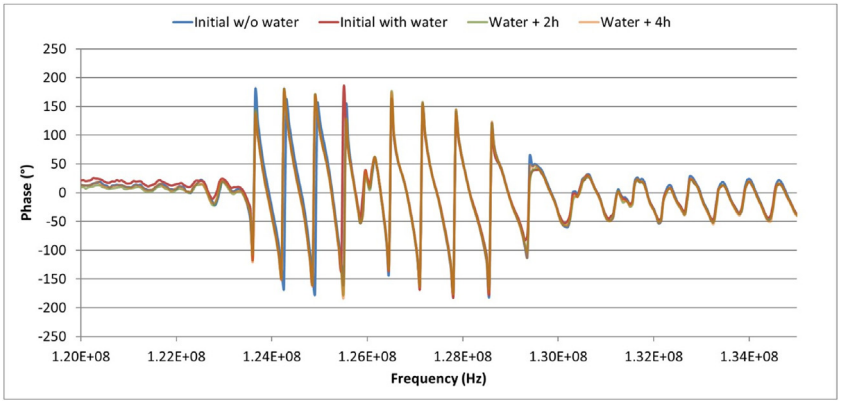

Fig. 13. Phase (S21) versus frequency range measured on the SAW sensor (#5) with and without DI water.

microfluidic channel in direct contact with the sensitive part of the SAW sensor. The result of this experiment are presented in Figs. 12 and 13.

Based on the results of the acoustic impedance characterization, we concluded that the processing steps involved in the assembly of the SAW sensor and sequential integration of the microfluidic channel, as well as its presence on the SAW sensor, has little or no impact of the assembled system performance. The analyses on the biofunctionalized samples are still ongoing and upon completion, we will report on the biofunctionalization technique and its effect on the SAW sensor frequency curve. The biofunctionalization of the sensing area makes it sensitive to specific biological elements in-liquid, such for example bacteria in complex liquids for an immunological detection.

7. Conclusion

In this work, we developed and demonstrated a simple, low-cost process for manufacturing a microfluidic device requiring no cleanroom. Micromilling technology was chosen for the microfluidic channel as it is a rapid, conceptually simple process and suitable not only for prototyping but also for low to medium scale production. This is in perfect match with niche market needs for the intended application. The microfluidic device was processed from polycarbonate (PC), it has an inlet and outlet, and a nominal volume of 13.2 μL. It has a well controllable wall thickness of less than 250 μm width. We demonstrated a room temperature process for the assembly of biofunctionalized surface acoustic wave (SAW) devices and subsequent device integration with the microfluidic

device to form a fully functional microfluidic biomedical detection system. The assembly and integration technique for a biofunctionalized SAW sensor is a carefully selected combination of known and matured processing steps that cause no damage to the sensitive biofunctionalization on the sensor. All materials and components used for the assembled microfluidic biomedical sensors system are compatible with biomedical devices.

We measured amplitude and phase of the acoustic impedance of the fully assembled microfluidic system in a frequency range from 115 MHz to 135 MHz. The results of an ultrasonic (US) impedance characterization show that neither the microfluidic system integrated on the sensor nor the integration process itself caused a detectable impact on the US impedance of the SAW sensor. This means that the microfluidic system does not affect the sensor performance.

CRediT authorship contribution statement

S. Stoukatch: Conceptualization, Methodology, Formal analysis, Investigation, Resources, Writing - original draft, Writing - review & editing, Visualization. **L.A. Francis:** Conceptualization, Validation, Writing - review & editing, Visualization, Project administration, Funding acquisition. **F. Dupont:** Methodology, Validation, Investigation, Resources, Writing - review & editing, Visualization, Supervision, Project administration. **M. Kraft:** Writing - review & editing, Funding acquisition.

Declaration of Competing Interest

The authors report no declarations of interest.

Acknowledgments

The authors would like to acknowledge contribution of all members Microsys lab, Department of Electrical Engineering and Computer Science, ULg (University of Liege), Belgium involved in the research and Sensors, Microsystems and Actuators Laboratory of Louvain (SMALL), ICTEAM Institute, Université Catholique de Louvain (UCL), Belgium for participation in the research and providing the samples.

The research has been carried out in the framework of the BIOBACTIL project, funded by the Walloon Region of Belgium (WB Health research program), Service Public de Wallonie (SPW), grant numbers: n° 1318026 and carried out by a consortium of research institutions.

References

[1] T.M.A. Gronewold, Surface acoustic wave sensors in the bioanalytical field: recent trends and challenges, Anal. Chim. Acta 603 (2) (2007) 119–128.
[2] E. Gizeli, E.G.E. Lowe (Eds.), Acoustic Transducers, Biomolecular Sensors, Taylor & Francis, London, 2002, pp. 176–206.
[3] N. Bracke, S. Barhdadi, E. Wynendaele, B. Gevaert, M. D'Hondt, B. De Spiegeleer, Surface acoustic wave biosensor as a functional quality method in pharmaceutics, Sens. Actuators B 210 (2015) 103–112.
[4] D.B. Go, M.Z. Atashbar, Z. Ramshani, H.-Ch. Chang, Surface acoustic wave devices for chemical sensing and microfluidics: a review and perspective, Anal. Methods 9 (28) (2017) 4112–4134, http://dx.doi.org/10.1039/C7AY00690J.
[5] T. Wang, R. Green, R. Guldiken, J. Wang, S. Mohapatra, S.S. Mohapatra, Finite element analysis for surface acoustic wave device characteristic properties and sensitivity, Sensors 19 (2019) 1749, http://dx.doi.org/10.3390/s19081749.
[6] J.-M. Friedt, L.A. Francis, Combined surface acoustic wave and surface Plasmon resonance measurement of collagen and fibrinogen layer physical properties, Sens. Biosensing Res. (2016), http://dx.doi.org/10.1016/j.sbsr.2016.05.007.
[7] L.E. Fissi, J.-M. Friedt, F. Chérioux, et al., Fabrication and packaging technologies of Love-wave-based microbalance for fluid analysis, Sens. Actuators A Phys. 162 (2) (2010) 304–309.
[8] L.E. Fissi, A. Jaouad, D. Vandormael, L.A. Francis, Fabrication of new interdigital transducers for surface acoustic wave device, Phys. Procedia (2015) 936–940.
[9] S. Stoukatch, Low-temperature microassembly methods and integration techniques for biomedical applications, in: Wireless Medical Systems and Algorithms, 2016, pp. 21–42.
[10] W.I. Wu, P. Rezai, H.H. Hsu, P.R. Selvaganapathy, Materials and methods for the microfabrication of microfluidic biomedical applications, in: X.-J.J. Li, Y. Zhou (Eds.), Microfluidic Devices for Biomedical Applications, Woodhead Publishing, 2013, pp. 3–62, http://dx.doi.org/10.1533/9780857097040.1.3.
[11] E.K. Sackmann, A.L. Fulton, D.J. Beebe, The present and future role of microfluidics in biomedical research, Nature 507 (March (7491)) (2014) 181–189, http://dx.doi.org/10.1038/nature13118, PMID: 24622198.
[12] M. Grösche, A.E. Zoheir, J. Stegmaier, R. Mikut, D. Mager, J.G. Korvink, K.S. Rabe, Ch.M. Niemeyer, Microfluidic chips for life sciences—a comparison of low entry manufacturing technologies, Small 15 (2019), 1901956, http://dx.doi.org/10.1002/smll.201901956.
[13] S. Van Loo, S. Stoukatch, F. Axisa, J. Destiné, N. Van Overstraeten-Schlögel, D. Flandre, O. Lefèvre, P. Mertens, Low temperature assembly method of microfluidic bio-molecules detection device, in: Proc. Low Temperature Bonding for 3D Integration (LTB-3D), 3rd IEEE International Workshop, Tokyo, 2012, pp. 181–184, May.
[14] X.-J.J. Li, Y. Zhou, Microfluidic Devices for Biomedical Applications, Elsevier Publisher, 2013, 676 p.
[15] L. Tang, J. Min, E.C. Lee, J.S. Kim, N.Y. Lee, Targeted cell adhesion on selectively micropatterned polymer arrays on a poly (dimethylsiloxane) surface, Biomed. Microdevices 12 (1) (2010) 13–21, http://dx.doi.org/10.1007/s10544-009-9353-1.
[16] G. Harman, Wire Bonding In Microelectronics, McGraw-Hill, M International, 2010, 446 p.
[17] Die Shear Strength, MIL-STD-883F, Method 2019.7.

Biographies

Serguei Stoukatch, Ph.D. in Electrical Engineering has 20+ years experience in Micro-assembly, Packaging and Interconnect Technology, among them: 4 years post-doctoral research at University of Gent, Belgium, 8 years at Interuniversity Microelectronics Centrum (IMEC), Leuven, Belgium, there he followed the career track starting from Process Engineer to Assembly Technology Section head and Senior Scientist. Currently he is a Senior Scientist at Microsys Laboratory, Liege University. He holds 2 patents and author/co-author more than 80 publications for professional conferences and technical journals. He is specializing in IC, microsystem, MEMS and biochip packaging; interconnect technology, and 3D integration.

Laurent A Francis received MS and PhD degrees from the Université Catholique de Louvain (UCL), Belgium, in 2001 and 2006, respectively. He is currently working as an Associate Professor at UCL. His research interests are related to co-integrated, ultra-low power CMOS MEMS sensors for biomedical applications and harsh environments. He was previously Researcher at IMEC in Leuven, Belgium, and a visiting Professor at the Université de Sherbrooke, Canada. He is author or co-author of more than 100 scientific articles, has co-edited one book and holds one patent. He is member of the Belgian National Committee on Biomedical Engineering and of the IEEE.

Francois Dupont received a MSc degree in Electrical and Electronics Engineering from the University of Liege, Belgium, in 2007. He subsequently joined the Microsys laboratory, University of Liege, as a research engineer in 2008. Since then, he has participated in about ten projects whose objectives were the integration/miniaturization of sensor systems. His core competence is the design of miniaturized and ultra-low power electronic circuit. From 2016, he team leader of the laboratory, whose research topics are energy harvesting, connected sensors system and advanced packaging.

Michael Kraft received a Dipl.-Ing. degree in electrical and electronics engineering from the Friedrich-Alexander University, Erlangen-Nürnberg, Germany, in 1993, and the Ph.D. degree from Coventry University, U.K., in 1997. He is currently a Professor of ESAT department, MICA group with the Catholic University of Leuven, Belgium. He has authored or co-authored over 200 peer-reviewed journal and conference papers. He has contributed to three textbooks on MEMS, and edited a book on MEMS for Aerospace and Automotive Applications. His research interests include MEMS and nanotechnology ranging from process development to system integration of MEMS and nano-devices.